In the over-broken and effectively broken ranges, as the ratio increases, the radius of the chip also increases. However, in the region where tangled chips are produced the trend reverses itself. In this region, the chip radius decreases as the ratio increases.

The results regarding the chip radius are interesting, but they do not provide much useful information for the machine operator who needs to know where to place a chip breaker to effectively control chips in a turning operation. In order to make the graph useful for this purpose, it has been broken down into three distinct regions by two vertical dashed line. The first line is located at the point where the ratio of breaker location to feed equals 13.5. To the left of this line the chips are over-broken. The second line is located at the point where the ratio is 29.5. To the right of this line the chips are all under-broken. Between these lines lies the region where effective breakage was noted. The transitions from one type of chip to another are very distinct. This indicates that the ratio of breaker location to feed is a good measure for predicting and adjusting breaker location for proper chip control when turning 4150 steel.

Conclusions

The data collected for this investigation indicates that it is possible to provide a practical means for a machine operator to predict where an obstruction type chip breaker should be placed for effective chip control when working with 4150 steel. The location of the breaker can be calculated using a ratio of breaker location to the feed which results in well-broken chips. Since the feed will have been set and is known to the operator, the proper breaker location can be calculated by multiplying the feed by the proper ratio. A good value of this ratio appears to be about 20, so for effective chip breaking with 4150 steel, the breaker should be located back from the primary cutting edge by a distance 20 times the feed. The beauty of this method is that the main cutting parameters need not be changed to get good chips. This means chip control is possible without decreasing the efficiency of the process significantly.

These experimental results also agree with the analysis in the sense that the ratio of the feed to the location of the chip breaker is indeed the most important parameter. The optimal ratio of chip breaker location to feed may also depend on other parameters such as tool geometry and materials as these variables affect the cutting process. However, for a given tool geometry and materials, properly broken chips can be obtained over various machining conditions by maintaining the ratio at a constant value.

References

1 Stabler, G. V., 1951, "The Fundamental Geometry of the Cutting Process," *Proc. Instn. Mech. Engr.*, 165, 14.

2 Henriksen, E. K., "Chip Breaking—a Study of Three Dimensional Chip Flow," *ASME Paper* No. 53-5-9.

3 Worthington, B., 1976, "A Comparative Literature Survey of Chip Control in Turning Process," *Proc. of the 17th Int. MTDR Conf.*, pp. 103–116.

4 Nakeyama, K., 1962, "A Study on Chip-Breaker," *Bulletin of JSME*, Vol. 5, No. 17, pp. 142–150.

5 Kluft, W., König, W., van Luttervelt, C. A., Nakayama, K., and Pekelharing, A. J., "Present Knowledge of Chip Control," *Annals of the CIRP*, Vol. 28, No. 2, pp. 441–453.

6 Jawahir, I. S., 1988, "The Tool Restricted Contact Effect as a Major Influencing Factor in Chip Breaking: An Experimental Analysis," *Annals of the CIRP*, Vol. 37, No. 1, pp. 121–126.

7 Shaw, M. C., 1984, *Metal Cutting Principles*, Oxford Press.

8 Jawahir, I. S., and Oxley, P. L. B., 1988, "New Development in Chip Control Research: Moving Towards Chip Breakability Predictions for Unmanned Manufacture," *Proc. of ASME Manufacturing International*, pp. 301–310.

9 Kane, G. E., 1971, "The Effect of Tool Geometry on Chip Breaking," *SME Technical Paper MR71-923*.

Vibration of Power Plant Piping

C. (Raj) Sundararajan[1]

Introduction

Piping systems in operating power plants are sometimes observed to have unusual vibrations. If unchecked, such sustained, low-amplitude vibrations can induce fatigue failures in pipes. One possible cause for such piping vibrations is the operation of rotating equipment such as pumps. If the frequency of operation of the equipment is close to a piping frequency, the piping system may vibrate in resonance with the equipment. Piping frequencies may be computed and compared with the equipment frequency, and if they match closely either the piping or equipment frequency shall be changed to avoid further vibrations. So a knowledge of the piping frequencies is necessary.

However, during power plant piping design, only static analyses are routinely carried out and piping frequencies are not computed (except in nuclear power plants). Though a number of piping vibration analysis computer programs are available, not every engineer who is doing piping design has such programs readily available at hand. The frequency analysis method presented in this technical note does not require a vibration analysis program; the fundamental frequencies are hand-calculated in just a few minutes using the static analysis results.

Methodology Development

Consider a three-dimensional piping system. A finite element model is developed, and $[K]$ and $[M]$ are the stiffness and mass matrices. Order of these square matrices is n, where n is the number of degrees of freedom. The mass matrix $[M]$ is developed on the basis of lumped-mass formulation.

An approximate solution to the fundamental frequency, using Rayleigh's method, is given by the following Eq. (1):

$$\omega^2 = \frac{\{\phi\}^T[K]\{\phi\}}{\{\phi\}^T[M]\{\phi\}} \tag{1}$$

where

ω = fundamental frequency of vibration,

$\{\phi\}$ = an assumed vibrational-mode vector which satisfies the boundary conditions (order of the vector is n; each element of the vector represents a degree of freedom of the piping system)

$\{\phi\}^T$ = transpose of $\{\phi\}$.

Any deformation vector which satisfies the boundary conditions is acceptable as $\{\phi\}$. Let us use the static deformation shape of the piping system due to gravity loads in the X-direction to compute the lowest frequency of vibration predominantly in the X-direction. Such a deformation shape is acceptable as the ϕ-vector since it satisfies all the boundary conditions. Similarly, the deformation shapes due to gravity loads in the Y and Z direction may be used to compute the lowest frequencies in the Y and Z directions, respectively.

Let the deformation shape due to gravity loads in the X-direction be represented by an nth order vector $\{\mathbf{u}\}$. This vector contains the deformations (displacements and rotations) of the n degrees of freedom due to gravity in the X-direction. Similarly, the deformation shapes due to gravity loads in the Y and Z directions are represented by $\{\mathbf{v}\}$ and $\{\mathbf{w}\}$, respectively.

[1]Consultant, Houston, TX.

Contributed by the Production Engineering Division for publication in the JOURNAL OF ENGINEERING FOR INDUSTRY. Manuscript received July 1991; revised Sept. 1991. Associate Technical Editor: S. C.-Y. Lu.

So an approximate solution to the lowest frequency in the X-direction (ω_x) is given by

$$\omega_x^2 = \frac{\{\mathbf{u}\}^T[K]\{\mathbf{u}\}}{\{\mathbf{u}\}^T[M]\{\mathbf{u}\}} \tag{2}$$

Lowest frequencies in the Y and Z directions (ω_Y and ω_Z, respectively) may also be computed similarly.

Equilibrium equation of the piping system subjected to gravity loads in the X-direction is given by

$$[K]\{\mathbf{u}\} = \{\mathbf{m}\}g \tag{3}$$

where g is the acceleration due to gravity and $\{\mathbf{m}\}$ is an nth order mass vector. Mass of the piping system at each node is placed at the vector element corresponding to the X-directional displacement degree of freedom of the piping system. All other elements of the vector are zero. So the right hand side of Eq. (3) represents the dead load at the different nodes due to gravity in the X-direction.

Substitution of Eq. (3) into Eq. (2) yields

$$\omega_x^2 = \frac{\{\mathbf{u}\}^T\{\mathbf{m}\}g}{\{\mathbf{u}\}^T[M]\{\mathbf{u}\}} \tag{4}$$

The numerator of Eq. (4) may be expanded as

$$\{\mathbf{u}\}^T\{\mathbf{m}\}g = \sum_{i=1}^{i=J} (m_i u_i g) \tag{5}$$

where J is the number of nodes, m_i is the mass at the ith node and u_i is the X-directional displacement at the ith node due to gravity loads in the X-direction.

Deflections in the Y and Z directions due to gravity loads in the X-direction are not necessarily zero but they will usually be small compared to the corresponding X-directional deflection. So the former deflections may be set to zero without introducing any significant error. With that approximation, denominator of Eq. (4) may be expanded as

$$\{\mathbf{u}\}^T[M]\{\mathbf{u}\} = \sum_{i=1}^{i=J} (m_i u_i^2) \tag{6}$$

Substitution of Eqs. (5) and (6) into Eq. (4) yields

$$\omega_x^2 = \frac{g \sum_{i=1}^{i=J} (m_i u_i)}{\sum_{i=1}^{i=J} (m_i u_i^2)} \tag{7}$$

Similarly,

$$\omega_Y^2 = \frac{g \sum_{i=1}^{i=J} (m_i v_i)}{\sum_{i=1}^{i=J} (m_i v_i^2)} \tag{8}$$

$$\omega_Z^2 = \frac{g \sum_{i=1}^{i=J} (m_i w_i)}{\sum_{i=1}^{i=J} (m_i w_i^2)} \tag{9}$$

Computations involved in Eqs. (7), (8), and (9) are simple and straightforward, and can be carried out quickly using a hand calculator.

Numerical Results

Accuracy of the method presented above is illustrated through a simple example.

The example piping system is shown in Fig. 1. The two end points of the piping system are fixed in all degrees of freedom. The horizontal and vertical pipes are connected by 90° short

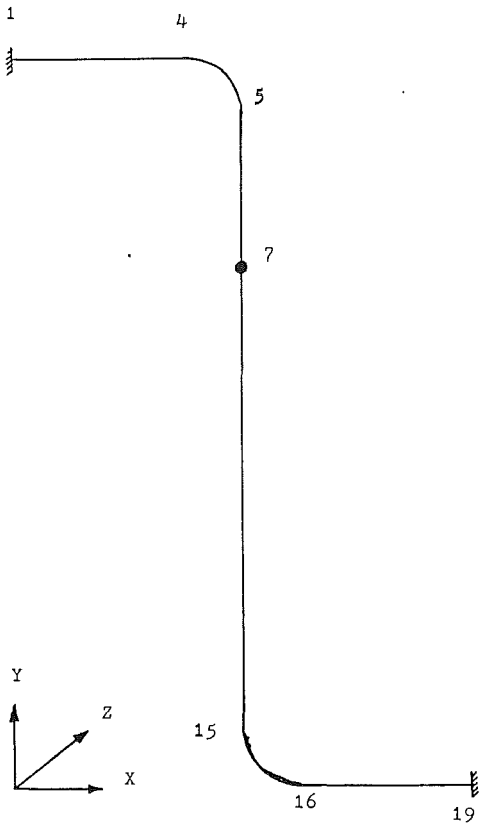

Fig. 1 Example piping system

Table 1 Nodal weights and displacements

NODE (i)	NODAL WEIGHT ($m_i g$)	u_i	w_i
1	21.7	0.0	0.0
2	43.3	0.00006	0.0009
3	43.3	0.0001	0.0027
4	57.7	0.0002	0.0051
5	101.0	0.0124	0.0188
6	130.0	0.0608	0.0588
7	1130.0	0.105	0.0959
8	130.0	0.136	0.122
9	130.0	0.152	0.135
10	130.0	0.155	0.136
11	130.0	0.143	0.125
12	130.0	0.120	0.104
13	130.0	0.088	0.0758
14	130.0	0.050	0.0435
15	101.0	0.010	0.0117
16	57.7	0.0001	0.0026
17	43.3	0.00007	0.0014
18	43.3	0.00003	0.0005
19	21.7	0.0	0.0

UNITS: $m_i g$ are in pounds, where g = 386.4 inch/sec^2
u_i and w_i are in inches

Table 2 Comparison of fundamental frequencies

Frequency	Present Method	Conventional Vibration Analysis	Percentage Difference
ω_X	58.05	57.73	0.554 %
ω_Z	61.47	61.44	0.049 %

NOTE: Frequencies are presented in radians/sec

radius elbows (radius = 8.464 in.). Each of the two horizontal runs are 24 in. long and the vertical run is 240 in. long. All pipes are 8 in. Sch. 40; that is, 8.625 in. outside diameter and 0.322 in. thickness. Modulus of elasticity is 27.9×10^6 psi and Poisson's ratio is 0.3. Self weight of the pipes including contents and insulation is 65 pounds per linear foot. A concentrated weight (representing a valve) of 1000 pounds is located at a distance of 48 in. below the upper elbow.

The piping system is discretized by a finite element model consisting of 18 elements and 19 nodes. Each of the two horizontal pipes is represented by 3 straight-pipe elements of 8 in. length each. The vertical pipe is represented by 10 straight-pipe elements of 24 in. length each. Each elbow is represented by an elbow element. Some of the node numbers are shown in Fig. 1. The concentrated weight is located at node 7. Nodal weights are given in Table 1.

Nodal deflections in the X-direction due to gravity loads in the X-direction (u_i) and nodal deflections in the Z-direction due to gravity loads in the Z-direction (w_i) are tabulated in Table 1. (These values are from static piping analyses for gravity loads.)

The lowest frequency of vibration predominantly in the X-direction (ω_X) and the lowest frequency of vibration predominantly in the Z-direction (ω_Z) are computed using Eqs. (7) and (9), respectively. These calculations are accomplished in a few minutes using a hand calculator. Frequencies thus computed are compared with frequencies computed via conventional, computerized frequency analysis (see Table 2). The present method gives remarkably accurate results.

Concluding Remarks

An approximate method of piping frequency calculations using the results of static analysis is presented in this paper. The necessary calculations can be carried out manually and quickly, and avoids the need for a formal, computerized frequency analysis.

The method is based on sound theoretical principles (based on the well-established and widely-used Rayleigh's method [1]). A judicious simplifying assumption, Eq. (6), eliminates the need for time-consuming quadratic, matrix computations, Eq. (4), and provides a simple formula, Eq. (7). An example piping system is analyzed using the method. The numerical results are very accurate (Table 2).

References

1 Clough, R. W., and Penzien, J., 1975, *Dynamics of Structures*, McGraw-Hill Book Company, NY.